AN APPROACH TO NUMERICAL SIMULATION AND ANALYSIS OF MOLTEN CORIUM COOLABILITY IN A BWR LOWER HEAD

C. T. Tran, P. Kudinov and T. N. Dinh

Nuclear Power Safety Division, Royal Institute of Technology
Roslagstullsbacken 21, Stockholm, Sweden, SE-106 91
thanh@safety.sci.kth.se; pavel@safety.sci.kth.se; namdinh@safety.sci.kth.se

Abstract

The paper discusses an application of the Computational Fluid Dynamics (CFD) method to support the development and validation of a computationally-affordable method named Effective Convectivity Model (ECM) for simulation of turbulent natural convection heat transfer and phase changes in a decay-heated corium pool in the Boiling Water Reactor (BWR) lower head. The CFD method simulations enable detailed study of separate-effect phenomena of corium flows. Insights gained from the CFD simulations, e.g. the heat flux profile along the vertical wall and the locally enhanced downward heat flux in the vicinity of the Control Rod Guide Tube (CRGT), are implemented in the ECM model and its extension, the PECM, for phase changes. The paper reports validation of the PECM model against experimental data, including SIMECO and LIVE experiments. Assessment of thermal loading on BWR vessel structures during severe accident progression using the PECM is performed and safety-relevant aspects are discussed.

1. INTRODUCTION

During the late phase of in-vessel accident progression, there is likelihood that a core melt pool will be formed in the reactor lower plenum. It is clear that in the case of core melt pool formation, predictions of melt pool characteristics and thermal loads on the vessel wall and reactor internal structures, as well as evaluations of the cooling measure effectiveness are of paramount importance for safety analyses. In order to perform such risk assessments, reliable and efficient tools are needed for simulations of melt pool heat transfer with high-fidelity prediction results.

Predictions of reactor scale melt pool characteristics and thermal loads are difficult tasks, especially for BWRs. There is a forest of CRGTs in the BWR lower plenum. The CRGTs can be used as a cooling measure by inside water flows to remove the heat from a melt pool. However, the presence of CRGTs makes geometry of the lower plenum complex. The main difficulties of reactor scale melt pool simulations are related to the high Rayleigh number (10^{15}-10^{17}) of a core melt pool, to the complex flow, specific geometry (e.g. BWR lower plenum) and long term transients of the accident progression.

The widely accepted engineering approach employing low-Reynolds number turbulence models (k-epsilon etc.) fail to predict energy splitting and heat flux distributions of a high-Rayleigh number core melt pool, Nourgaliev and Dinh (1997). The Direct Numerical Simulation (DNS) CFD method provides capability for analysis of thermal hydraulics and gaining insights into turbulent natural convection. However, the DNS method is computationally expensive. DNS can not be used for simulation of long transient (tens hours) flow and heat transfer of a melt pool in the real BWR lower head geometry. Nonetheless, CFD methods have been used for revealing flow physics and examining separate-effect phenomena. Previously, Dinh et al. (1997) performed CFD simulations to assess the significance of some selected effects, including variations in melt properties, pool geometry and heating conditions. The common approach is to conduct simulant material experiments and to generalize experimental data in the form of correlations. In general, small-scale core melt experiments are difficult to apply, as a result of the heating methods, geometry representation, low value of Rayleigh number *Ra* and other measurement and

test performance difficulties. Analytical and computational modeling has not yet proved to be reliable enough to describe turbulent natural convection and heat transfer of a large volumetrically heated pool in the lower plenum. The highest priority should be given to the separate-effect phenomena that could have the largest effect on the heat fluxes imposed on the melt pool boundary.

Historically, majority of experimental correlations on natural convection heat transfer were obtained with water (Pr = 7) or freon (Pr ~ 8-12). In the later work of Nourgaliev et al. (1997), the effect of the relatively low Prandtl number of corium (Pr ~ 0.1-0.6) on heat transfer characteristics in internally heated liquid pools (rectangular, semicircular and elliptical cavity configurations) was numerically studied. The effect of Pr number on *Nu* number at the bottom surface is found to be significant and it increases with the increase of *Ra* number.

For engineering analysis, simplified models are needed to predict heat transfer of a melt pool. Cheung et al. (1992) developed the model of effective diffusivity and used to solve analytically heat transfer in a horizontal heat-generating layer. The Effective Convectivity Conductivity Model (ECCM) was first introduced in by Bui and Dinh (1996), implemented in the code named MVITA and reported in detail by Sehgal et al. (1998). The lumped parameter method used in the severe accident codes MELCOR 1.8.6 (2005) and MAAP (1999), as well as in the studies of Park and Dhir (1992), and Dombrovskii et al. (1998), is an effective approach for solving heat transfer of a melt pool. Also, the Finite Element Method (FEM) in the COUPLE solver, using the effective thermal conductivity combined with the local heat transfer model of the SCDAP/RELAP5-3D, seems to be an effective tool for simulations of heat transfer of a melt pool, being capable to describe natural convection and dynamics of the phase-change boundary of a pool in 2D geometry (SCDAP/RELAP5/MOD3, 2003). Willschuetz et al. (2006) implemented the effective conductivity model in ANSYS code to simulate melt pool heat transfer in conjunction with thin boundary layers surrounding a debris bed as a tool to correct temperature profile and energy splitting. However, due to specific limitations, these simplified models are not suitable for solving melt pool heat transfer in the real geometry of a BWR lower plenum.

Thus there is a necessity to develop a new tool which is computationally-affordable and sufficiently-accurate to be able to capture flow physics for simulations of accident progression in the real BWR lower plenum geometry. In the present study, we formulate an approach and show a way of effective usage of CFD for solutions of Nuclear Reactor Safety (NRS) problems, namely heat transfer and coolability of a corium pool in the BWR lower head. The technical approach is delineated in Fig. 1.

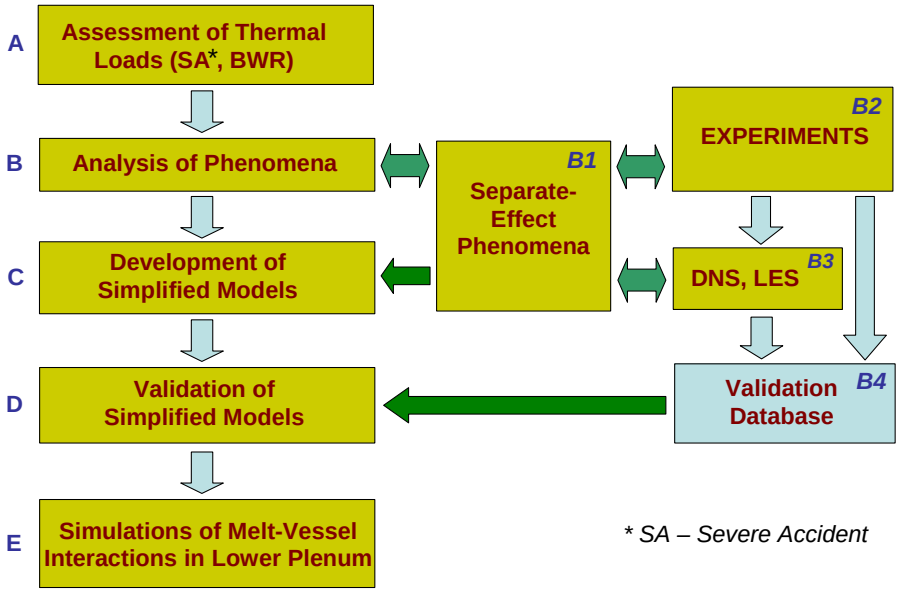

Fig. 1: A technical approach to solutions of core melt pool heat transfer in a BWR lower head.

The main task is assessment of thermal loadings on the vessel wall and structures during the late phase of in-vessel accident progression in a BWR (Fig. 1, A). At the first stage we realized that due to complicated, long transient physical phenomena and complex geometry, the CFD methods are not directly applicable for solving of heat transfer of a core melt pool in the BWR lower head. Thus, development of computationally efficient and reliable models is a must for solution of the problem.

At the second stage (Fig. 1, B, B1), the analysis of physical phenomena involved in the BWR corium pool heat transfer shows that important separate-effect phenomena can be the descending flows along the cooled CRGT walls (boundary layers), the flow impingement on the vessel wall in the vicinity of CRGTs.

Then (Fig. 1, B2, B3, B4) using available experimental data and performing CFD simulations for specific BWR lower head geometries, we examine separate-effect phenomena, generating database for development and validation of models. For attaining this purpose, we employ the **Fluent** code. Experiments provide data for validation of the CFD tool (from B2 to B3).

Based on the insights gained from the experiments and CFD simulations, the simplified computationally effective models ECM and PECM were developed (Fig. 1, C). The simplified model reflects the local effects of heat transfer and enables use of experimentally obtained heat transfer coefficients (a correlation-based simplified model). The ECM (and PECM) is implemented in **Fluent** using User Defined Functions (UDF). Using a commercial CFD code as a vehicle allows us to take advantages of the code pre- and post processing tools including the Adaptive Mesh Refinement (AMR) technique.

The key step is validation of the simplified model (Fig. 1, D) with a dual-tier approach, i.e. against experimental data and data provided from CFD simulations. Finally, the validated simplified model is applied for simulations of melt-vessel interactions in real geometry of the BWR lower head with a forest of CRGTs (Fig. 1, E).

The paper material is presented as follows. In Section 2, results of CFD simulations are presented. The basics of the ECM method (the ECM and PECM) and its validation are introduced in Section 3. In Section 4, an application of the ECM method to simulations of melt pool formation heat transfer in BWR lower plenum geometry is presented. A summary and safety-relevant key finding conclude the paper.

2. CFD SIMULATIONS AND INSIGHTS INTO FLOW PHYSICS

2.1. CFD method and grid convergence study

The methods of DNS and Large Eddy Simulations (LES) are powerful tools to analyze turbulent flows in detail (Grotzbach and Worner, 1999). A suggestion was made on that LES is the most promising and efficient approach to numerical simulations in both Rayleigh-Benard fluid layers and volumetrically heated liquid pools, as well as to intensive applications to the thermal fluid-structure interaction problems. A series of previous publications (Dinh and Nourgaliev, 1997), demonstrated that anisotropy is the utmost important factor in understanding and modeling of high Rayleigh-number thermal convection.

The CFD method used in the present study is a high-resolution grid method to effectively provide large eddy simulations without an explicit Sub-Grid Scale (SGS) model (“no model” LES method). To effectively capture wall-boundary effects, a much higher resolution grid is provided in the near-wall region of the computational domain. Numerical simulations for different unstably stratified thermal flows using the “no model” LES showed that the method works quite well in predicting mixing and heat transfer of natural convection in volumetrically heated liquid pools and for transient cool-down liquid pools (Nourgaliev et al., 1997). An analysis of past works as well as a review of recent advances in turbulence modeling and simulation revealed that an empirical selection of numerical schemes for use in “no model” LES method of turbulent natural convection in internally-heated liquid pools has a root in Monotonically Integrated LES (or MILES) method (Boris et al, 1992). This CFD method is validated against the existing experimental data, and results of the CFD simulations are well agreed with the experimental data (±15%) for a wide range of Rayleigh number (10^8-10^{14}) (Tran and Dinh, 2007).

A grid convergence study is performed for a volumetrically heated fluid (core melt) layer cooled from the top in 3D geometry. As it is shown in Fig. 2, grid convergence can be obtained for the predicted heat transfer coefficients. Although, we have to mention that the demand for the grid resolution is growing with increase of *Ra* number. Grid resolution required for convergence in a wide range of *Ra* number is presented in Fig. 3. All results of CFD simulations presented in the paper are obtained with a grid resolution which provides grid convergent solutions.

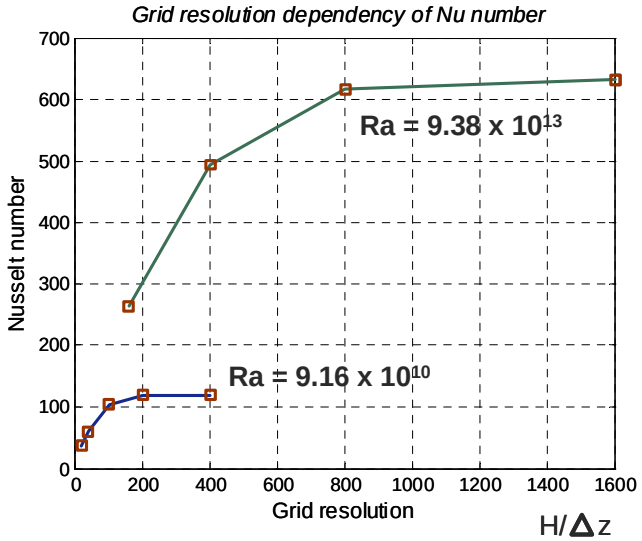

Fig. 2: Grid resolution dependence of heat transfer coefficients.

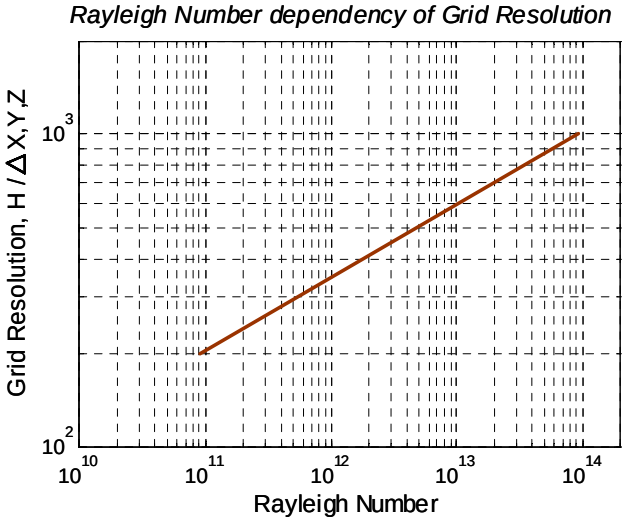

Fig. 3: Rayleigh number dependence of required grid resolution ($H/\Delta X,Y,Z$).

2.2. CFD simulation of flow and heat transfer in a BWR lower plenum unit volume

We define the unit volume as a rectangular cavity surrounding one CRGT. In the case of core melt pool formation in the BWR lower plenum, natural convection in the pool is driven by buoyancy force of decay-heated liquid and downward boundary layer flows along cold surfaces of CRGTs and the vessel wall. Due to a large number of CRGTs (hundreds) in the lower plenum, it is reasonable to assume that the flow pattern in the unit volume is only slightly affected by the large scale circulation flow in the pool. In this case, the unit volume can be considered as representative characteristic geometry of the BWR lower plenum. Flow pattern and heat transfer inside the unit volume completely define heat exchanges between

the pool, the CRGTs and the vessel wall. Thus understanding of unit volume heat transfer is a key for prediction of corium melt pool heat transfer.

In the present work, the CFD simulation is performed for a unit volume of 0.3126x0.3126x0.4 m. The diameter of the CRGT is 0.1245 m. Isothermal boundary conditions are applied to the top, CRGT and bottom walls. A fine grid with cell sizes of less than 0.5 mm is provided along the cooled boundaries where temperature gradients are high. Fig. 4 shows contours of the velocity and temperature. It is seen that a well-mixed region and a stratified region are formed respectively in the upper part and lower part of the volume. A boundary layer is formed along the CRGT. The heat flux along the CRGT is higher in the upper part (Fig. 5). In the prevalent part of the CRGT, the heat flux profile obeys the boundary layer development concept which produced the following heat transfer correlation (Chawla and Chan, 1982):

$$Nu_{side} = 0.508\ \mathrm{Pr}^{1/4}\left(\frac{20}{21}+\mathrm{Pr}\right)^{-1/4} Ra_y^{1/4} \qquad (1)$$

The heat flux analytically derived from eqn. (1) is described graphically in Fig. 5 as the analytical model.

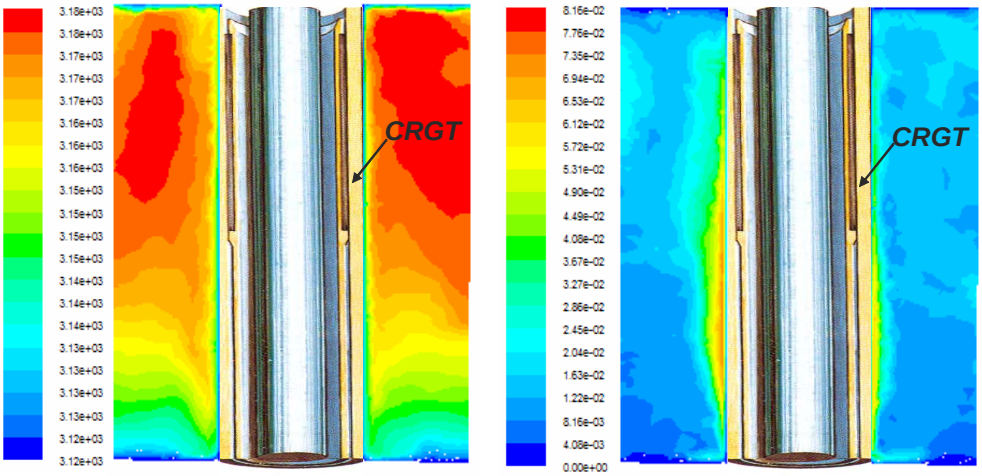

Fig. 4: Unit volume CFD simulation, contours of temperature (left) and velocity (right).

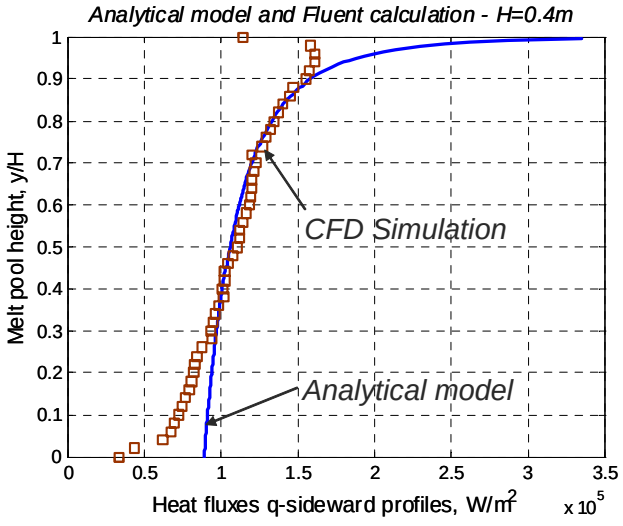

Fig. 5: Profile of heat transfer along a cooled vertical wall and boundary layer concept.

The analysis of the downward heat flux revealed a locally enhanced heat flux surrounding the CRGT (Fig. 6). The enhancement of the heat flux is related to the low fluid Prandtl number (Pr = 0.6) effect which was previously studied by Nourgaliev and Dinh (1997). Additional simulations performed for higher Prandtl numbers (for the same Rayleigh number and mesh) show that with increasing of Pr number the effect is getting weaker. As shown in the figure, for Pr = 18, the effect is almost disappeared.

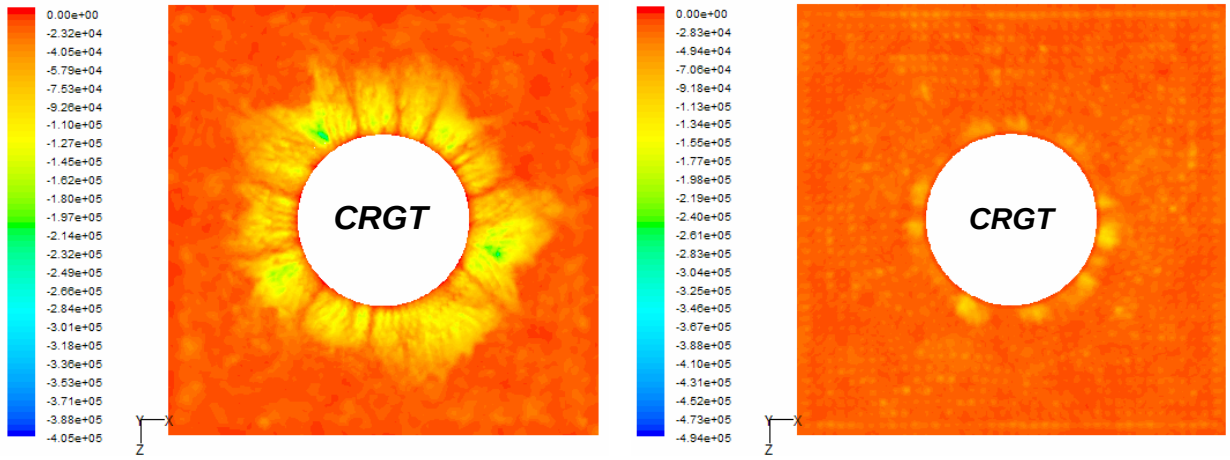

Fig. 6: Contours of downward heat fluxes for different Prandtl numbers: Left Pr=0.6; Right Pr=18.

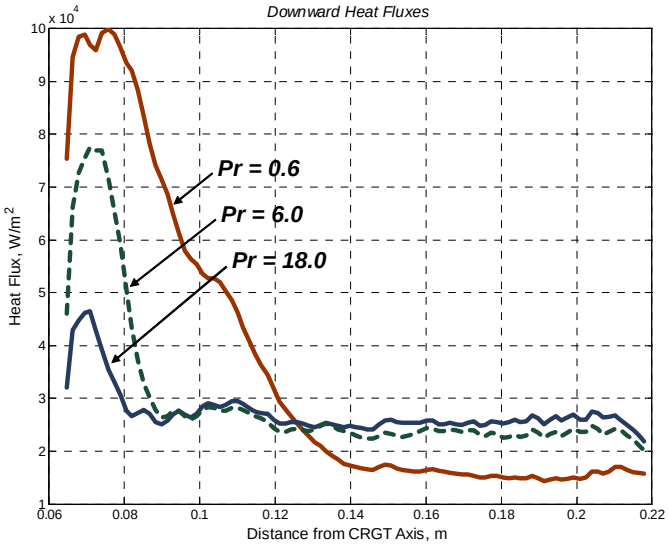

Fig. 7: Surface-averaged downward heat flux profiles of different Pr numbers.

The effect of low Pr number on the downward heat flux is shown clearer in Fig. 7. In the region close to the CRGT, the heat flux is almost sixfold of that in the outside region for the case of Pr = 0.6. The downward heat flux is not only increased locally (in the vicinity of the CRGT), but the surface average values of the downward heat flux are also increased, although not very much. Table 1 gives values of the upward, sideward (i.e. to the CRGT) and downward heat fluxes calculated from CFD simulations for three different Prandtl numbers. While the upward and sideward heat fluxes are almost unchanged, the downward heat flux of Pr = 0.6 is increased for 29% compared with the case of Pr = 18.

We suppose that the enhancement of the downward heat flux may threaten the vessel integrity. Without external vessel cooling, high downward heat fluxes from the corium pool would cause a rapid ablation of the Reactor Pressure Vessel (RPV) wall. Most importantly, the impingement of the flow descending along

the CRGT cooled wall may cause local vessel melt-through leading to melt discharge as a film along the ex-vessel part of the control rod driver.

Table 1: Steady state surface-averaged heat fluxes and pool temperature of different Pr number cases

Parameters	Pr = 0.6	Pr = 6.0	Pr = 18.0
Pool temperature, K	3164.11	3157.26	3232.28
Upward heat flux, W/m^2	167110	162640	159994
Sideward heat flux, W/m^2	108156	113536	115405
Downward heat flux, W/m^2	**34879**	**28601**	**27051**

As it has been shown, the CFD simulations provide profiles of the sideward heat flux and locally enhanced downward heat flux surrounding the CRGT. The obtained profiles were implemented in the developed simplified ECM model which is used to simulate melt pool heat transfer of a real BWR lower plenum configuration.

3. THE ECM METHOD

3.1. The ECM method introduction

The ECM method advanced the concept of the Effective Convectivity Conductivity Model (ECCM) of Bui and Dinh (1996). The ECM method uses only the effective convectivity model implemented in the **Fluent** through UDF. The detailed description of the ECM is presented in Tran and Dinh (2007). Later on, the ECM was extended to Phase-change problems, so called PECM, which is described in detail by Tran and Dinh (2007). For the readers to follow more easily, we present a short introduction to the ECM and PECM.

In the ECM and PECM we do not solve Navier-Stokes equations. The following heat transfer equation is solved as a conduction equation:

$$\frac{\partial}{\partial t}\left(\rho C_p T\right) = \nabla \bullet \left(k \nabla T\right) - \frac{\partial\left(\rho \Delta H\right)}{\partial t} - \nabla \bullet \left(\rho u C_p T\right) - \nabla \bullet \left(\rho u L\right) + Q_v \tag{2}$$

The ECM method uses the directional characteristic velocities U_{up}, U_{down} and U_{side} instead of the fluid velocity u, to describe convective terms of equation (2). The characteristic velocities are derived using energy balance equations, and presented through heat transfer coefficients as follows:

$$U_{up} = \frac{\alpha}{H_{pool}} \times \left(Nu_{up} - \frac{H_{pool}}{H_{up}} \right) \tag{3}$$

$$U_{side} = \frac{\alpha}{H_{pool}} \times \left(Nu_{side} - \frac{2 \times H_{pool}}{W_{pool}} \right) \tag{4}$$

$$U_{down} = \frac{\alpha}{H_{pool}} \times \left(Nu_{down} - \frac{H_{pool}}{H_{down}} \right) \tag{5}$$

where H_{pool} is the depth of the melt pool, H_{up} is the depth of the pool upper mixed region; H_{down} is the depth of the lower stratified region; W_{pool} is the pool width. The H_{pool} and W_{pool} are taken from the transient values of the formed pool during simulation, H_{up} (and H_{down}) is assumed to be as follows:

$$H_{up} = \frac{H_{pool} \times Nu_{up}}{Nu_{up} + Nu_{side} + Nu_{down}} \quad (6)$$

In the ECM, the Steinberner-Reineke correlations (Steinberner and Reineke, 1978) are used to calculate Nu_{up} and Nu_{down}. The sideward Nusselt number Nu_{side} is defined using equation (1).

As it is seen, the defined characteristic velocities are always positive, this means that an artificial amount of energy is added into computational domain during one time step of simulation. This additional amount of energy has to be extracted in the next step of simulation. A numerical technique is applied to extract the artificial added energy using UDF of **Fluent**.

For a mushy region, the characteristic velocity values depend on the fluid fraction. It is possible to implement different models of fluid fraction dependence of a mushy velocity. Having the possibility of implementing the fluid velocity in a mushy zone, the ECM method enables description of natural convection heat transfer of a mushy zone, thus enables simulations of melt pool formation heat transfer.

3.2. Validation of the ECM and PECM

The ECM and PECM tools were validated against experimental data and the data obtained from CFD simulations (a dual approach) as shown in Table 2.

Table 2: Data used for validation of the ECM and PECM

Validated tools	Experimental and CFD simulation data	Descriptions
ECM	Kulacki-Emara experiment	Fluid layer cooled from the top wall
	Kulacki-Goldstein experiment	Fluid layer cooled from the top and bottom walls
	Unit volume CFD simulation	Unit volume cooled from the top, CRGT and bottom walls
PECM	SIMECO experiment, 1998	Circular segment of eutectic $NaNO_3$-KNO_3 melt, cooled from the top surface and vessel wall
	LIVE-L1 experiment, 2006	Semispherical plenum of non-eutectic $NaNO_3$-KNO_3 mixture, cooled by an external water flow

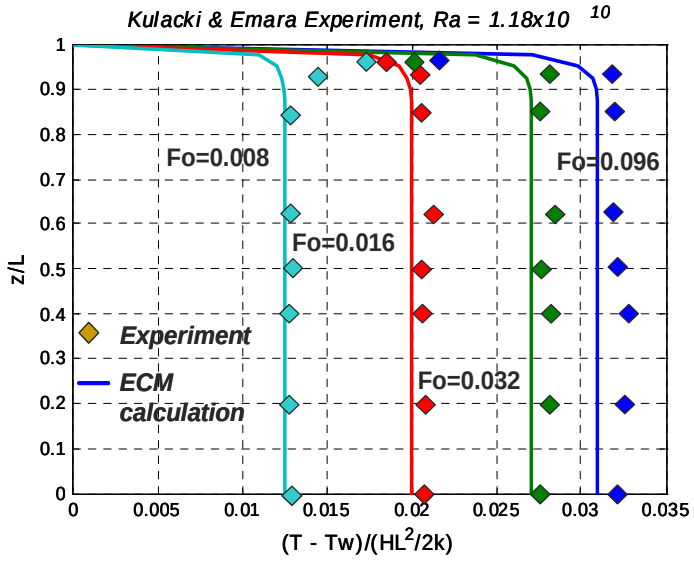

Fig. 8: Transient temperature profiles of ECM simulations vs. Kulacki-Emara experiment data (Note to the figure: *Tw* is top wall temperature, *H* is the heat source and *L* is the thickness of fluid layer).

Experimental data used for validation of the ECM include (i) transient temperature profiles of Kulacki & Emara (1977) with fluid layer cooled from the top; and (ii) experiment of Kulacki & Goldstein (1972) with fluid layers cooled from the top and bottom. Fig. 8 shows good agreement of the ECM simulation and experimental transient temperature profile. Also, as it is shown in Fig. 9, the ECM simulation well predicts temperature profiles of fluid layers cooled from the top and bottom.

The CFD simulation method, in the one hand is a good tool for prediction of flow thermal hydraulics, on the other hand provides data for validation of developed simplified models. Fig. 10 shows predicted by the CFD and ECM heat flux distributions along the CRGT of a unit volume. The profiles are well agreed. It is worth noting that the ECM allows large time steps, compared to those of the CFD simulation. More importantly, the ECM effectiveness is obtained by the much lower number of iterations needed to achieve solution convergence in each time step. So the ECM (and PECM also) simulation is 100-200 times faster than the CFD simulation. The ECM simulation does not require a fine grid.

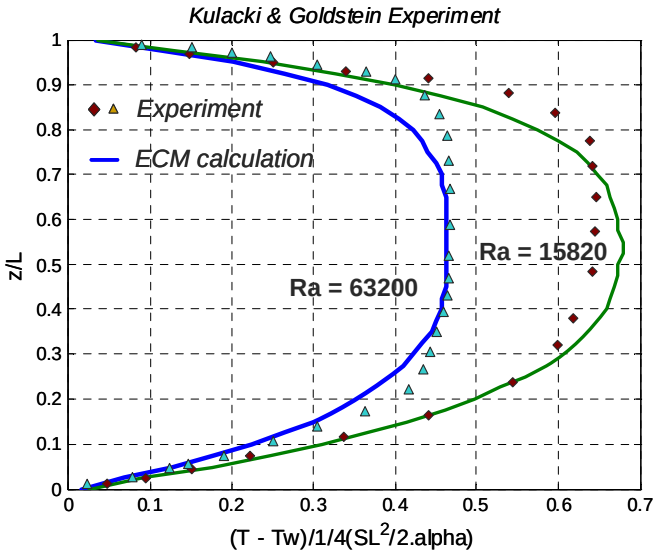

Fig. 9: Temperature profiles of ECM calculations vs. Kulacki-Goldstein experimental data (Note to the figure: *Tw* is wall temperature, *S* is the heat source, *L* is the thickness of fluid layer, *alpha* is α).

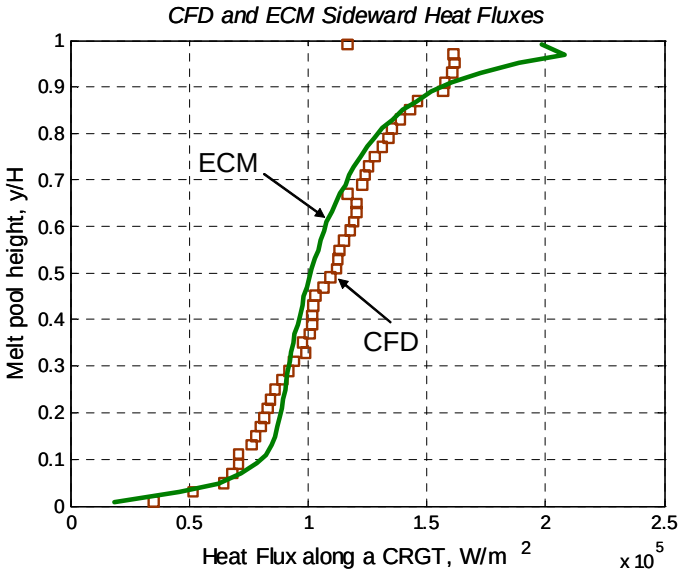

Fig. 10: Heat flux distributions along the tube wall (Unit volume CFD and ECM simulations).

For the PECM tool validation, the SIMECO experiment which was performed at KTH, NPS (Sehgal et al., 1998), and the LIVE-L1 experiment which was recently performed at FZK, Germany (Miassoedov et al., 2007) are used.

The SIMECO experiments were conducted in a slice-type facility as shown in Fig. 11. Both eutectic and non-eutectic binary salt mixtures of KNO_3-$NaNO_3$ were used. The PECM is validated against the experiment with a eutectic mixture (SSEu-10).

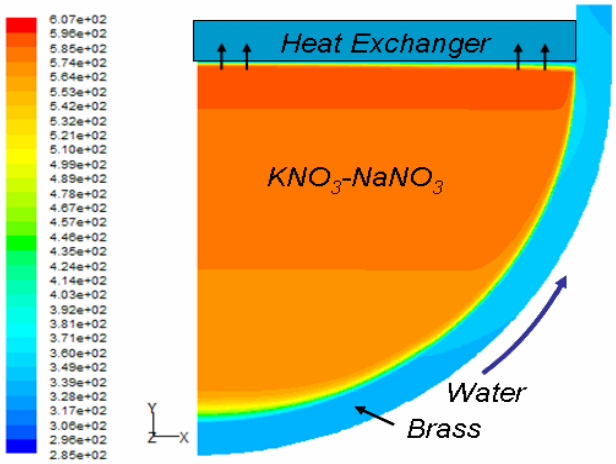

Fig. 11: SIMECO experiment, temperature contour (in K, middle plane).

The following boundary conditions were implemented: the pool top surface is cooled by heat exchangers so isothermal boundary condition is used; the angular brass surface is cooled by water coming from the lower part, so convection heat transfer boundary condition is applied; the back wall is insulated, and the front wall is made of a special glass for visualization so a small heat flux of about 10-20 W/m^2 is applied for this wall. The initial temperature is 300K.

Good agreement of the PECM simulation results and the experimental data was obtained: the vertical temperature profiles are shown in Fig. 12 and the vessel wall heat flux distributions in Fig. 13.

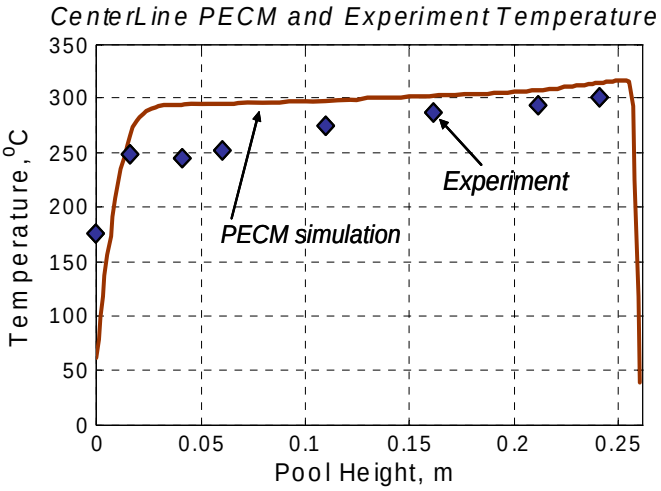

Fig. 12: Temperature profile along the pool centerline: PECM vs. experiment.

Slightly higher temperature and heat flux are observed in the PECM simulation compared with the experiment in the lower region of the pool. The PECM predicted temperature profile is more flat compared with the experiment, resulting in higher temperature in the lower region that causes a thinner crust, as a result the heat flux is increased. A larger experimental crust thickness of the lower region may

be explained by two other probable reasons: more cold liquid is accumulated in this region from all the upper inclined surfaces of the crust, or the effect of non-uniformed heated volume of the experiment (electrically heated) compared with the uniformly heated volume of the PECM simulation that causes an accumulation of cold liquid to be solidified in this region. The possible effect of accumulation of cold liquid in the lower region is difficult to be reflected in a simplified model. Also, the heat loss during the experiment may contribute an additional deviation to the data.

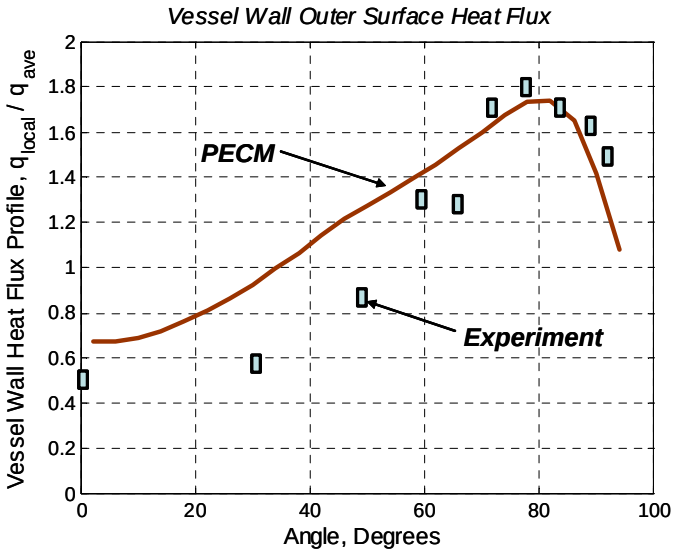

Fig. 13: Vessel wall heat flux distribution (PECM vs. experiment).

The LIVE-L1 experiment was performed in a stainless steel semispherical plenum with a radius of 0.4966 m. The simulant used is non-eutectic mixture of KNO_3 and $NaNO_3$ (80%-20%). The purpose of the experiment is to investigate the core melt behavior in the vessel with outside cooling. At the beginning, the melt of 350 ^oC is poured into the plenum which is cooled outside by the air. The electrical heating system heats up the melt to higher temperature for 2 hours, afterward steel vessel cooling by a water flow is initiated. The electrical power input into the melt was changed during the experiment and the crust thickness was measured for a steady state condition.

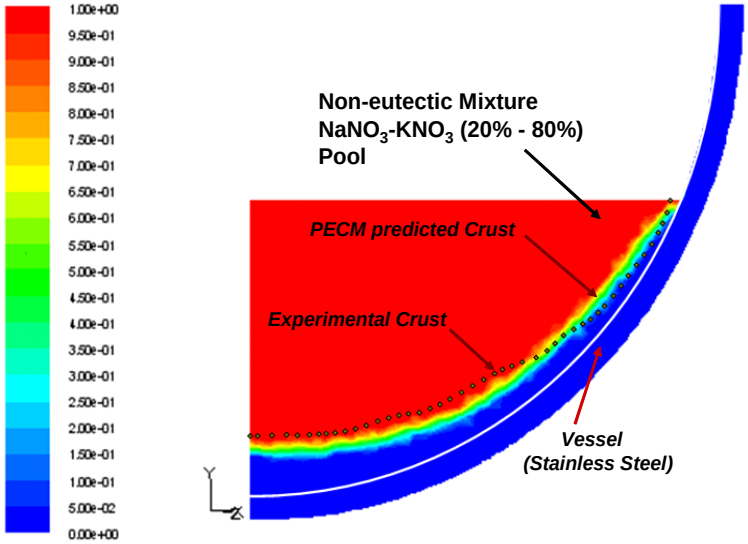

Fig. 14: PECM prediction of crust thickness (LIVE – L1 experiment, FZK).

The PECM well captures the pool behavior. Fig. 14 shows the crust thickness of the experiment, together with crust thickness predicted by the PECM. As it is shown, the PECM result is reasonably well agreed with the experiment. Crust thickness of the PECM simulation in the lower region is thinner compared with the experimental (58.97 mm vs. 70.67 mm in the lowermost region) that can be explained as previously for the SIMECO experiment simulation. This difference seems to be insignificant compared with the possible experimental uncertainty which is related to the heat loss from the melt pool top surface. In addition, the other possible reason leading to the crust thickness difference is the different heating power distribution to the six layers of the melt pool. In the upper region of the melt pool, due to a high peaked heat flux of the boundary layer model implemented in the PECM, crust is not formed.

The results of simulations show that the PECM is a suitable, efficient tool for prediction of melt pool heat transfer. In the next Section, the PECM tool is applied to BWR configuration melt pool simulations.

4. ANALYSIS OF SEVERE ACCIDENT PROGRESSION IN A BWR LOWER PLENUM

Applications of the ECM and PECM to simulations of melt pool formation heat transfer in a BWR lower plenum were reported by Tran and Dinh (2007, 2008). Here we present an example of PECM application to analysis of the corium Prandtl number effect discussed in Section 2 on accident progression.

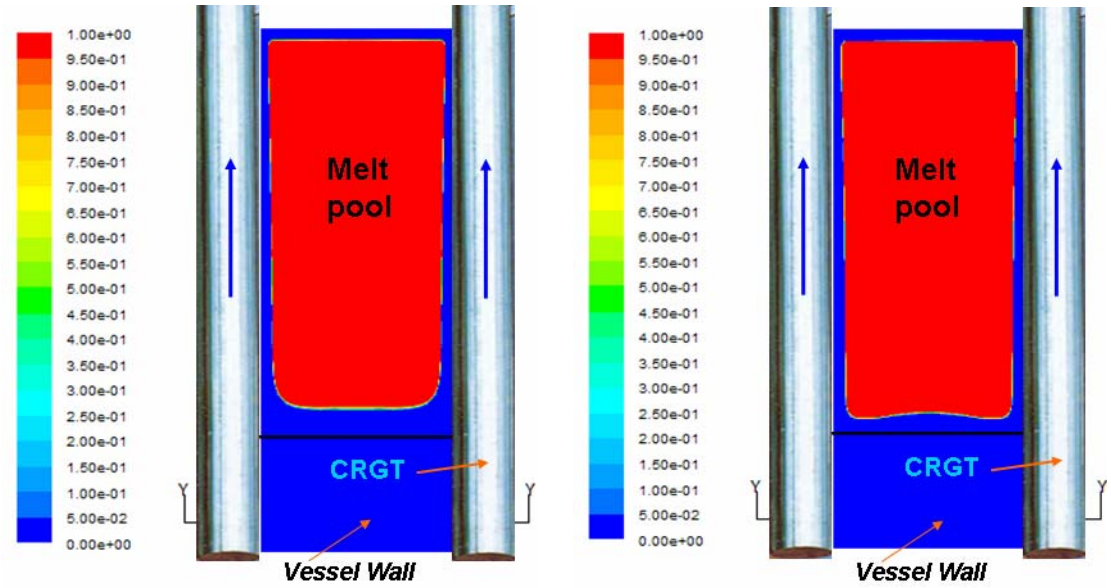

Fig. 15: Melt pool formation and crust (The left is the PECM with a correlation-based downward heat flux; the right is the PECM with an enhanced peaking downward heat flux).

Considering a 0.7 m height unit volume connected below with the vessel wall, the PECM tool is used for two cases: a case with a normal downward heat flux (correlation-based only) and a case with a locally enhanced downward heat flux. Assuming the core melt pool is homogeneous and the decay heat is $1MW/m^3$, Rayleigh number of such a melt pool in the ABB-Atom reactor lower plenum (diameter of 3 m) reaches $2x10^{14}$. To evaluate the possibility of vessel failure under thermal loading, we can accept the thermal creep limit temperature of 1000 ^oC, based on the report of Rempe et al. (1993).

The top surface of the debris bed and CRGTs are cooled by water, the interface of the debris bed and vessel wall is coupled, in reality, the external surface of the vessel wall is insulated, so a small heat flux (about $20W/m^2$) is allowed. Due to presence of small gaps in-between the CRGT walls and the vessel wall, this interface is applied to radiation or air conduction heat transfer. The other surfaces are applied either to adiabatic or symmetrical boundary conditions. Simulations are initiated with a dry-out condition of the debris bed (cake), the initiation bed temperature is about 450K.

Fig. 15 and 16 show the melt pool and crust in the lower plenum in connection with CRGTs, and the temperature contour. The locally enhanced downward heat flux causes a thinner crust between the melt pool and the vessel wall, especially in the places close to CRGTs. However, the heat flux is not high enough to ablate all crust covering the vessel wall. The vessel wall's temperature is additionally increased compared with the correlation-based downward heat flux case. The plot of the maximum vessel wall outer surface temperature shows a slight increase of 80-90 ^{o}C for the case with a locally enhanced downward heat flux (Fig. 17). Although the temperature increase acts to accelerate vessel failure due to thermal creep, the effect of low fluid Pr number is not as strong as we previously supposed.

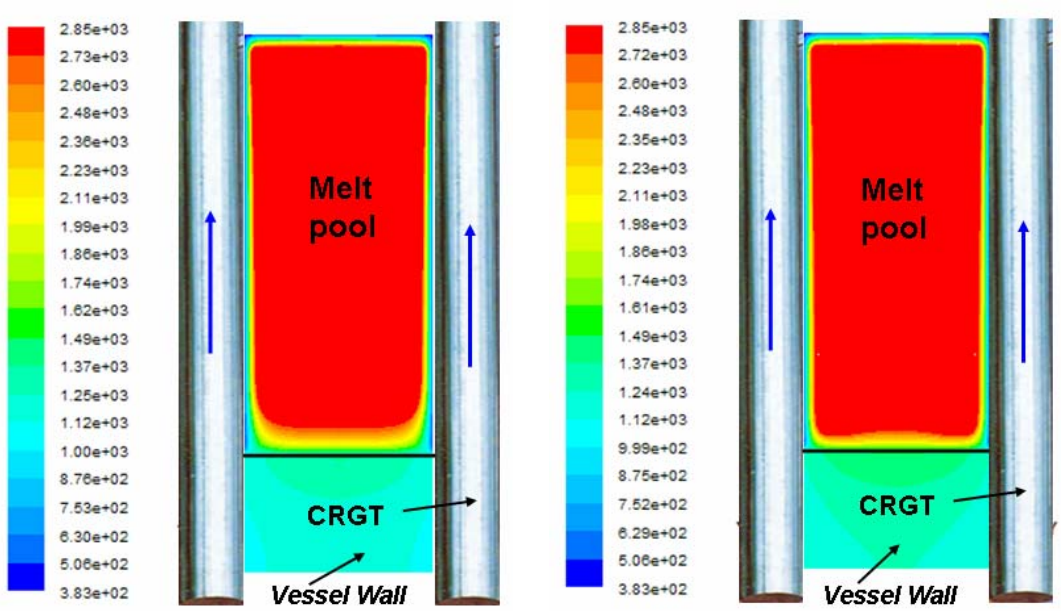

Fig. 16: Temperature contours in K of the pool and vessel wall (The left is the PECM with a correlation-based downward heat flux; the right is the PECM with an enhanced peaking downward heat flux).

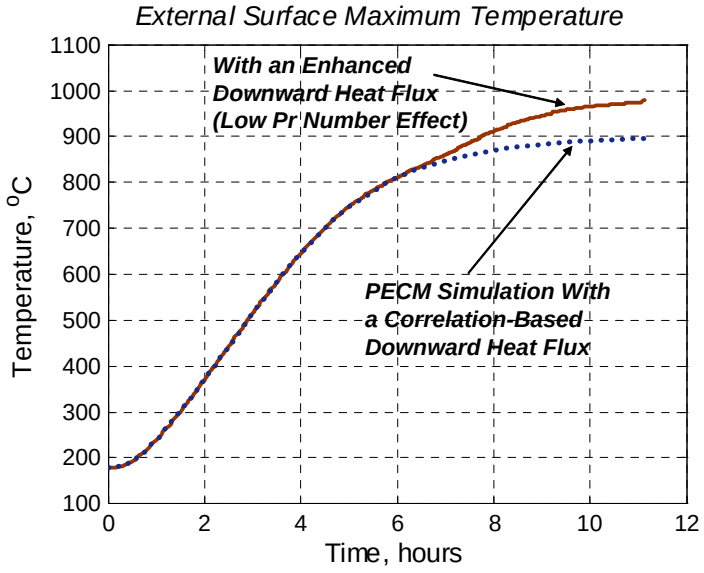

Fig. 17: Effect of low Prandtl number on vessel wall temperature evolution (Unit volume simulation).

The increase of vessel temperature is assumed to be insignificant compared with other uncertainties such as mass of the molten pool and chemical compositions. However, the significance of the additional

temperature increase is envisioned as it is related to the two safety-relevant reasons. The first, for a melt pool of 0.7 m depth, the steady state temperature of the vessel wall already reaches the thermal creep limit. An additional increase in temperature will make the vessel wall more sensitive to the creep rapture. The second reason is that this increase in temperature is a local effect, which may result in changing of the lower head vessel failure mode (e.g. the failure position). In turn, this change results in different discharged melt mass and flow rate which significantly affects the ex-vessel accident progression.

5. CONCLUDING REMARKS

An approach for effective application of CFD to a BWR safety problem has been presented. The CFD is used to examine separate-effect phenomena as well as to provide data, supporting the development and validation of a simplified model, called the Effective Convectivity Model (ECM). The ECM and its extension, Phase-change ECM (PECM) are implemented in the **Fluent** code and validated against experimental and CFD simulation data. The developed model is found to be sufficiently accurate and computationally efficient for simulations of transient processes of melt pool formation in the BWR lower plenum's complex geometry during a hypothetical severe accident.

Most interestingly, the CFD simulations for oxidic corium melts exhibit a locally enhanced downward heat flux in the region around the CRGT. The effect is attributed to the corium's Prandtl number. The locally enhanced downward heat flux implemented in the PECM shows a minor additional heatup of the BWR vessel wall. The temperature increase may accelerate vessel failure. Additional simulations and analyses are needed to clarify the creep acceleration and the change of the vessel failure position.

6. NOMENCLATURE

Arabic

C_p	Specific heat capacity, J/(kg.K)
Fo	Fourier number, $Fo = \frac{t \times \alpha}{H^2}$
g	Gravitational acceleration, m/s^2
H	Height of a volume or fluid layer, depth of a melt pool, m
k	Thermal conductivity, W/(m.K)
L	Latent heat of the phase change, J/kg
Nu	Nusselt number, $Nu = \frac{qH}{k\Delta T}$
Pr	Prandtl number, $\Pr = \nu / \alpha$
q	Heat flux, W/m^2
Q_v	Volumetric heat source, W/m^3
Ra	Rayleigh number (internal), $Ra = \frac{g\beta Q_v H_{pool}^5}{k\nu\alpha}$
Ra_y	Local Rayleigh number, $Ra_y = \frac{g\beta\Delta T y^3}{\nu\alpha}$
S_c	Source term, W/m^3
t	Time, s
T	Temperature, K
U	Characteristic velocity, m/s
u	Fluid velocity, m/s
W	Width of a volume, m
y	Local vertical coordinate, m

Greek

α	Thermal diffusivity, m^2/s, $\alpha = \frac{k}{\rho . C_p}$
β	Thermal expansion coefficient, 1/K
ΔH	Latent heat, J/kg
ΔT	Temperature difference, K
ΔZ	Grid cell size, m
ρ	Density, kg/m^3
ν	Kinematics viscosity, m^2/s

Subscripts and superscripts

down	Downward
pool	Pool
side	Sideward
up	Upward
x, y, z	Coordinate axis directions

7. REFERENCES

J. P. Boris, F. F. Grinstein, E. S. Oran and R. L. Kolbe, "New Insights into Large Eddy Simulation", *J. Fluid Dynamics Research*, **Vol. 10**, pp. 199-228, 1992.

V. A. Bui and T. N. Dinh, "Modeling of Heat Transfer in Heated-Generating Liquid Pools by an Effective Diffusivity-Convectivity Approach", *Proceedings of 2nd European Thermal-Sciences Conference*, Rome, Italy, pp. 1365-1372, 1996.

T. C. Chawla and S. H. Chan, "Heat Transfer From Vertical/Inclined Boundaries of Heat-Generating Boiling Pools", *J. of Heat Transfer*, **Vol. 104**, pp. 465-473, 1982.

F. B. Cheung et al., "Modeling of Heat Transfer in A Horizontal Heat-Generating Layer by An Effective Diffusivity Approach". *ASME HTD*-**Vol. 192**, pp. 55-62, 1992.

T. N. Dinh and R. R. Nourgaliev, "Turbulence Modeling for Large Volumetrically Heated Liquid Pools", *Journal of Nuclear Engineering and Design*, **Vol. 169**, pp. 131-150, 1997.

T. N. Dinh, R. R. Nourgaliev, and B. R. Sehgal, "On Heat Transfer Characteristics of Real and Simulant Melt Pool Experiments", *Journal of Nuclear Engineering and Design*, **Vol. 169**, pp. 151-164, 1997.

L. A. Dombrovskii, L. I. Zaichik, and Yu. A. Zeigarnik, "Numerical Simulation of The Stratified-Corium Temperature Field and Melting of The Reactor Vessel for A Severe Accident in A Nuclear Power Station", *Thermal Engineering*, **Vol. 45**, No.9, pp. 755-765, 1998.

R. O. Gauntt et al., "MELCOR Computer Code Manual, Core (COR) Package Reference Manuals", *NUREG/CR-6119, Vol. 2, Rev.2*, Version 1.8.6, , September 2005.

G. Grotzback, M. Worner, "Direct Numerical and Large Eddy Simulations in Nuclear Applications", *International Journal of Heat and Fluid Flow*, **Vol. 20**, pp.222-240, 1999.

F. A. Kulacki and A. A. Emara, "Steady and Transient Thermal Convection in a Fluid Layer with Uniform Volumetric Energy Sources", *J. Fluid Mech.*, **Vol. 83**, part 2, pp. 375-395, 1977.

F. A. Kulacki and R.J. Goldstein, "Thermal Convection in a Horizontal Fluid Layer with Uniform Volumetric Energy Sources", *J. Fluid Mech*. **Vol. 55**, part 2, pp. 271-287 (1972).

"MAAP4 Users Manual", *Fauske Associated Inc.*, Vol. 2, 1999.

A. Miassoedov, T. Cron, J. Fiot, S. Schmidt-Stiefel, T. Wenz, I. Ivanov, D. Popov, "Results of the LIVE-L1 Experiment on Melt Behavior in RPV Lower Head Performed within the LACOMERA Project at the Forschungszentrum Karlsruhe", *Proceedings of 15th International Conference on Nuclear Engineering Nagoya (ICONE)*, Japan, April 22-26, 2007.

R. R. Nourgaliev, T.N. Dinh and B.R. Sehgal, "Effect of Fluid Prandtl Number on Heat Transfer Characteristics in Internally Heated Liquid Pools with Rayleigh Numbers up to 10^{12}", *Journal of Nuclear Engineering and Design*, **Vol. 169**, pp. 165-184 (1997).

R. R. Nourgaliev, T. N. Dinh, and B. R. Sehgal, "Simulation an Analysis of Transient Cooldown Natural Convection Experiments", *Journal of Nuclear Engineering and Design*, **Vol. 178**, pp.13-27, 1997.

R. R. Nourgaliev and T. N. Dinh, "An Investigation of Turbulence Characteristics in an Internally-Heated Unstably-Stratified Fluid Layer", *Journal of Nuclear Engineering and Design*, **Vol. 178**, pp.235-258, 1997.

H. Park, V. Dhir, "Effect of Outside Cooling on the Thermal Behavior of a Pressurized Water Reactor Vessel Lower Head", *J. of Nuclear Technology*, **Vol. 100**, pp. 331-346, December 1992.

J. L. Rempe, S. A. Chavez, G. L. Thinnes, C. M. Allison, G. E. Korth, R. J. Witt, J. J. Sienicki, S. K. Wang, L. A. Stickler, C. H. Heath, S. D. Snow, "Light Water Reactor Lower Head Failure Analysis", *NUREG/CR-5642, EGG-2618*, Idaho National Engineering Laboratory, USA, 1993.

SCDAP/RELAP5-3D Code Development Team, "SCDAP/RELAP5-3D© Code Manual", *Report INEEL/EXT-02-00589, Revision 2.2*, Idaho National Engineering and Environmental Laboratory, October 2003.

B. R. Sehgal, V. A. Bui, T. N. Dinh, J. A. Green, G. Kolb, "SIMECO Experiments on In-Vessel Melt Pool Formation and Heat Transfer with and without a Metallic Layer", *Proceedings of In-Vessel Core Debris Retention and Coolability Workshop*, Garching, Germany, March 3-6, pp. 205-213, 1998.

B. R. Sehgal, V. A. Bui, T. N. Dinh and R. R. Nourgaliev, "Heat Transfer Process in Reactor Vessel Lower Plenum during A Late Phase of In-Vessel Core Melt Progression", *J. Advances in Nuclear Science and Technology*, Plenum Publ. Corp., 1998.

U. Steinberner and H. H. Reineke, "Turbulent Buoyancy Convection Heat Transfer with Internal Heat Sources". *Proceedings of the 6th Int. Heat Transfer Conference*, Toronto, Canada, Vol.2, pp. 305-310 (1978).

C. T. Tran, T. N. Dinh, "An Effective Convectivity Model for Simulation of In-Vessel Core Melt Progression in Boiling Water Reactor", *2007 International Congress on Advances in Nuclear Power Plants (ICAPP 2007)*, Nice Acropolis, France, May 13-18, 2007.

C. T. Tran and T. N. Dinh, "Simulation of Core Melt Pool Formation in a Reactor Pressure Vessel Lower Head Using an Effective Convectivity Model", Proceedings, *International Topical Meeting on Nuclear Reactor Thermal Hydraulics – NURETH-12*, Pittsburgh, Pennsylvania, USA, September 30 – October 04, 2007.

C. T. Tran and T. N. Dinh, "Application of the Phase-change Effective Convectivity Model to Analysis of Core Melt Pool Formation and Heat Transfer in a BWR Lower Head", *Transactions of ANS 2008 Annual Meeting*, Anaheim, California, USA, June 8-12, 2008.

H.-G. Willschuetz, E. Altstadt, B. R. Sehgal, F.-P. Weiss, "Recursively Coupled Thermal and Mechanical FEM - Analysis of Lower Plenum Creep Failure Experiments", *Annals of Nuclear Energy,* **Vol. 33**, pp. 126-148, 2006.